

DETAILED STUDY OF MILLIMETER WAVE EBG GUIDE: BROADBANDING TECHNIQUES, MODAL STRUCTURE, AND CROSSTALK BEHAVIOR

Yaser S. E. Abdo^{1,*}, M. R. Chaharmir², J. Shaker², and Y. M. M. Antar³

¹National Institute for Standards, Egypt

²Communications Research Centre Canada, Canada

³Royal Military College of Canada, Canada

Abstract—An electromagnetic band gap (EBG) waveguide using holes drilled in a dielectric substrate is investigated in this paper. A broadbanding technique is suggested and implemented through a detailed study of the modal behaviour of the guiding structure. The stop band of the EBG waveguide was adjusted by changing the width of the waveguide to increase its bandwidth. It is shown that the propagating mode is a quasi-TEM by examining the dispersion properties of the propagating mode. An EBG waveguide of 49.1 mm (equivalent to 19 EBG cells) was designed and fabricated. The simulation results show better than -10 dB return loss performance from 27 GHz to 31.5 GHz with insertion loss of better than 2.5 dB over the same bandwidth, and also high isolation in the range of -20 dB with an adjacent similar EBG waveguide. There is a good agreement between the measured data and simulation results. A microstrip line was also fabricated and used as a benchmark for comparison with the designed EBG waveguide. The group velocity of this waveguide is nearly constant across its operating frequency band which implies low frequency dispersion and is also a confirmation of the quasi-TEM nature of the EBG fundamental mode. Also, using the physical insight gained from a careful study of the EBG guide, a simple method is suggested for the calculation of the dispersion characteristic of its fundamental mode.

Received 20 February 2013, Accepted 1 April 2013, Scheduled 2 April 2013

* Corresponding author: Yaser S. E. Abdo (yaserabdo76@gmail.com).

1. INTRODUCTION

Electromagnetic band gap (EBG) structures are artificial periodic structures prohibiting the propagation of electromagnetic waves of certain polarizations at certain frequencies and directions [1]. These periodic structures are known as photonic bandgap (PBG) or photonic crystals in optical sciences and have been used for controlling light. Recently EBG structures have been used for microwave and millimeter-wave applications to enhance the radiation pattern of antennas [2], and also to realize broadband components [3]. An EBG waveguide can be created by introducing a 1-D perturbation/defect in the periodic lattice of an EBG structure. If electromagnetic waves with frequencies within the band gap are launched into the defect region, they will be well confined due to the cladding effect of EBG and guided along the defect region. EBG waveguides have been used to design different devices working in optics such as: directional couplers [4, 5], wavelength-division demultiplexers [6, 7], and wave splitters [8]. Since an EBG structure is used as a sidewall of the EBG waveguide, it could provide a high isolation between adjacent EBG waveguides, which gives an advantage to EBG waveguide when used in the design of MM wave components.

A square lattice of dielectric rods and a triangular lattice of holes have been used to design EBG waveguides, and the perturbation to realize the 1-D defect has been implemented by varying the size of one row of air holes or dielectric rods in the EBG substrate as described in [9]. An EBG waveguide with metal vias to excite TE_{10} mode in microwave band was also introduced in [10]. In this paper, an EBG waveguide is designed using a square lattice of air holes sandwiched between two metal plates, and taking into consideration the special case of completely filled holes in order to create the defect region. Using holes rather than metal vias in the realization of the EBG waveguide lowers the conductor losses, especially at high frequencies, and simplifies the fabrication process. An EBG waveguide that is easy to fabricate has been designed using a triangular lattice of holes which doesn't have a complete bandgap was recently reported [11]. A square lattice of holes has been used before to design an EBG waveguide at microwave bands [12, 13], but the measured insertion loss of these structures showed a stop band which reduced the bandwidth of the designed waveguides. Alternatively, this paper presents a physical insight into the modal characteristics of EBG guides and using this knowledge to overcome limiting factors towards its broadband operation.

The EBG substrate which has a bandgap for TM modes (magnetic

field parallel to the substrate surface and perpendicular to the holes [1]) around 30 GHz is designed in Section 2. The dispersion diagram of this EBG material is calculated for the irreducible Brillouin zone. Subsequently, in Section 3, the EBG waveguide is constructed using the designed EBG substrate by filling in the central row of the holes. The simulated transmission characteristics are obtained using CST Microwave Studio [14]. The projected band structure of the proposed EBG waveguide is calculated to study the coupling between different guided modes, and to determine the nature of the fundamental guided mode at 30 GHz. This projected band structure is used to optimize the designed structure and increase its bandwidth. A time domain solver [14] is used to calculate dispersion properties of the designed EBG waveguide. The obtained dispersion properties of the EBG waveguide indicate that the guided mode within the EBG waveguide is a quasi-TEM mode. A full wave simulation of the designed structure is done to show electric and magnetic fields of the fundamental guided mode. Two adjacent EBG waveguides are simulated to calculate the crosstalk between them. A microstrip line operating at 30 GHz is used as a benchmark to evaluate the performance of the designed EBG waveguide. The validation results show wideband operation from 27 GHz to 31.5 GHz and a high confinement of the guided electromagnetic wave within the guiding region.

2. DESIGN OF EBG STRUCTURE AND EBG GUIDE

The EBG structure is targeted to operate around 30 GHz, therefore, the EBG is to be synthesized to have a band gap around 30 GHz. The EBG structure is constructed using square lattice of holes within a dielectric substrate of dielectric constant $\epsilon_r = 10.2$ and thickness $h = 0.64$ mm (c.f. Figure 1). To achieve an electromagnetic band gap for *TM* modes around 30 GHz [15] which is essential for the realization of an EBG guide in the same band, the hole radius-to-unit cell size ratio (r/a) is chosen to be 0.48 to obtain a wide band gap.

To ensure that this EBG material has a band gap around 30 GHz along all the directions of the square lattice, the dispersion diagram should be calculated along the three sides of the irreducible Brillouin zone triangle. A unit cell of the proposed EBG structure was used to calculate the dispersion diagram by applying a periodic boundary condition on the sides of the unit cell and PEC on the top and bottom faces. All simulations were carried out using the commercial software CST [14]. The resulting dispersion diagram is shown in Figure 3. It is obvious that there is a band gap between first and second modes that occurs within the normalized frequencies, $0.24 < \omega a/2\pi c < 0.32$.

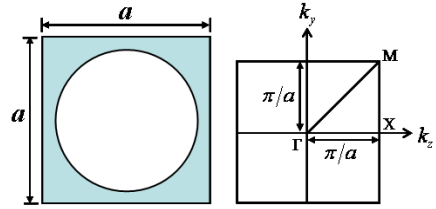
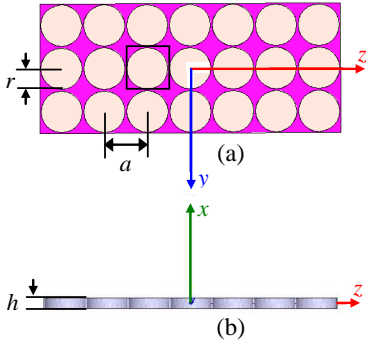


Figure 1. A square lattice of holes which has a unit cell size a ; (a) top view, and (b) side view.

Figure 2. Unit cell and irreducible Brillouin zone for the square lattice.

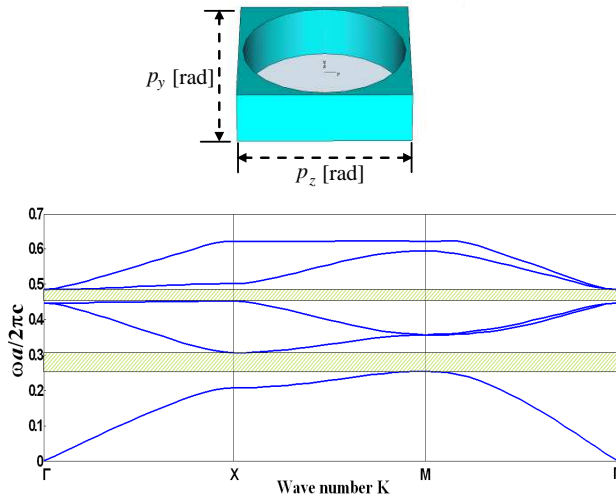


Figure 3. A unit cell and a dispersion diagram of the EBG structure.

The calculated dispersion diagram was exploited to design the EBG substrate for operation at 30 GHz. The unit cell size a can be calculated from the normalized frequency, shown in Figure 3, to locate the centre frequency, 30 GHz, within the bandgap. Following this procedure, a unit cell size of 2.583 mm was calculated to achieve this objective and hence the hole radius r is equal to 1.24 mm. This value of the unit cell size makes the square lattice of holes to have a bandgap from 25 GHz to 35 GHz. This EBG substrate will be used to design an EBG waveguide.

3. EBG WAVEGUIDE DESIGN

The proposed EBG waveguide can be created by removing a central row of holes along z direction of the EBG that was studied in the previous section. The projected band structure of the EBG waveguide can be calculated to ensure that the guided mode is located within the band gap of the EBG structure. Since the propagation of the guided mode is along z -axis, the eigenmodes that could propagate through the EBG material along Γ - X direction (see Figure 2) can be determined by varying the phase difference along z direction, p_z , from 0 to π for a specific value of the phase difference along y direction, p_y . Varying p_y from 0 to π results in the dark regions illustrated in Figure 4. Electromagnetic modes locating within these dark regions can leak into the EBG structure. To calculate the defect mode which is the mode guided within the defect region of the EBG waveguide, EBG waveguide is modelled by including a single cell along z -axis and 21 unit cells along y -axis. The defect was placed at the center by removing one hole as shown in Figure 4, so that the the width of the channel W_g is equal to $(2a - 2r = 2.69 \text{ mm})$. Periodic boundary conditions were applied in z direction to capture periodicity of the lattice along this direction. The guided modes within the EBG waveguide can be calculated by varying phase difference in the direction of periodicity of the waveguide and

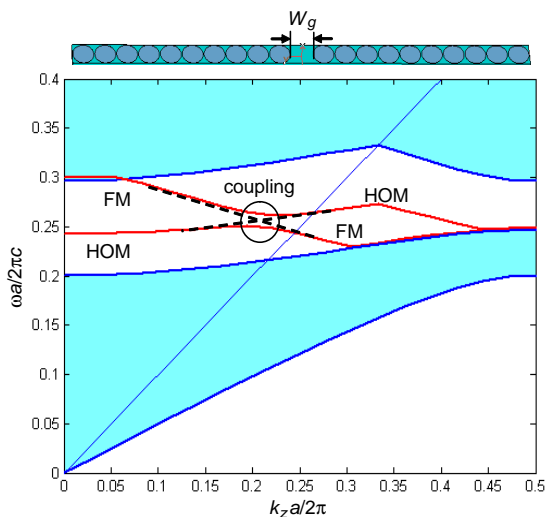


Figure 4. A unit cell and the projected band structure of the EBG waveguide.

calculate the corresponding modal frequency. From superimposing the dispersion characteristics of these guided modes on the projected band structure diagram of the EBG as shown in Figure 4 one can check if the defect modes are located within the band gap of the EBG.

Figure 4 shows the fundamental guided mode (FM) and the higher order mode (HOM) of the EBG waveguide. This higher order mode, which cuts the middle of the bandgap, is similar to Fabry-Perot modes due to the existence of the surrounding EBG crystal [16]. The fundamental mode covers the whole bandgap from the upper edge to the lower one. Since both of these two modes are getting closer to each other at a normalized frequency of 0.26 (intersection point) there is a contra-directional coupling between these guided modes. Two dashed lines, shown in Figure 4, were drawn to illustrate the contra-directional coupling process. Figure 5 shows the E -field pattern of the guided mode before and after coupling, respectively. The higher order mode has a TM nature and still can be guided within the EBG waveguide as illustrated in Figure 5(b). This contra-directional coupling can give rise to a mini-bandgap around a normalized frequency of 0.26 which corresponds to 30.5 GHz due to the flatness of the guided modes, and hence the bandwidth of the EBG waveguide is limited below this mini-bandgap.

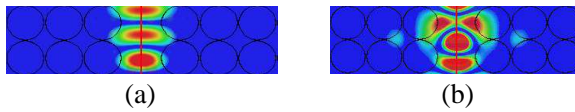


Figure 5. An E -field pattern of the guided wave, (a) before coupling, (b) after coupling.

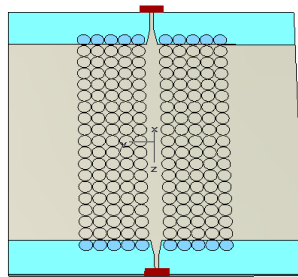


Figure 6. A designed EBG waveguide by removing the central row of holes.

The structure of the EBG waveguide is shown in Figure 6. Two metal plates were placed on the top and bottom of the EBG substrate. The length of the EBG waveguide is 19 unit cells long, which is equal to 49.1 mm. A microstrip-to-waveguide tapered transition was employed in order to excite the EBG waveguide [17]. The width of the microstrip line was set to 0.7698 mm in order to maintain $50\ \Omega$ matching. The design of this type of transition was realized by optimizing the feature sizes using CST microwave studio, transition width and transition length which were optimized to 3 mm and 2.0667 mm, respectively. The length of the feeding microstrip line is 4.5 mm.

The simulated S -parameters of the designed structure, shown in Figure 7, indicate a stop band from 29.5 GHz to 31 GHz. The calculated projected band structure in Figure 4 illustrates that this stop band, around 30.5 GHz, is due to the coupling between the fundamental mode and a higher order mode.

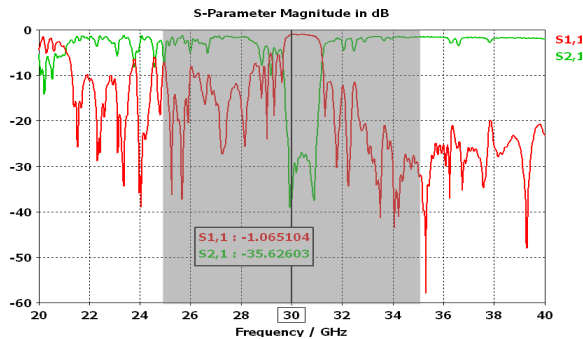


Figure 7. Simulated S -parameters of the designed EBG waveguide (the shadowed area shows the bandgap of the square lattice of holes).

The mini-stop band of the designed EBG waveguide, shown in Figure 6, limits the waveguide operation around 30 GHz as can be seen from Figure 7. To increase the bandwidth and to get better transmission characteristics for the EBG waveguide, the width of the EBG waveguide is decreased to 2 mm. By decreasing the width of the EBG waveguide, the proportional volume of the total dielectric in the EBG guide is decreased and the modes are shifted towards the air band and away from the dielectric band, i.e., toward higher frequencies and hence the coupling between the fundamental and the higher order modes occurs around the normalized frequency of 0.28 which corresponds to 33.5 GHz as illustrated by the calculated projected band structure shown in Figure 8. The EBG waveguide after decreasing its width was simulated. It is obvious from the simulated

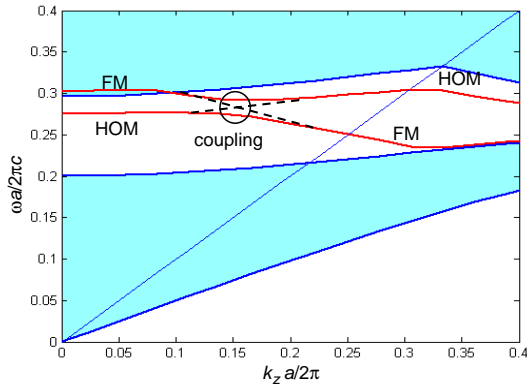


Figure 8. The projected band structure of EBG waveguide after decreasing its width.

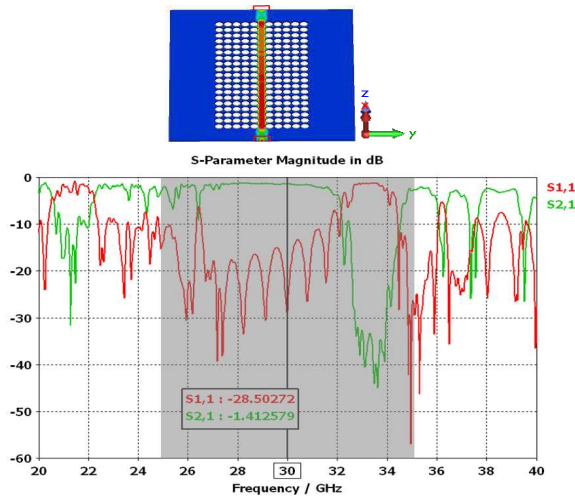


Figure 9. A simulated EBG waveguide after decreasing its width and its S -parameters (the shadowed area shows the bandgap of the square lattice of holes).

S -parameters, shown in Figure 9, that the mini-stop band is shifted to around 33.5 GHz which is consistent with the projected band structure. As shown in Figure 9 the guided wave is well confined within the EBG waveguide as required. A good transmission coefficient with insertion loss better than 2.5 dB was obtained for 27 GHz to 31.5 GHz band as observed in this figure. The return loss is also better than -10 dB

throughout the bandwidth, which demonstrates the possibility of using this EBG waveguide across a 4.5 GHz bandwidth in the Ka-band.

To study the dispersion properties of the EBG waveguide, a time domain analysis was carried out using CST time domain solver [14]. The group delay was calculated and the result is shown in Figure 10 which shows a constant value across the band of the EBG waveguide. This indicates a linear group velocity and consequently low dispersion for the EBG waveguide.

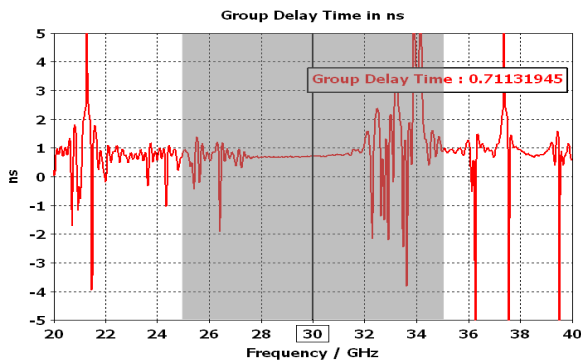


Figure 10. The group delay of the EBG waveguide (the shadowed area shows the bandgap of the square lattice of holes).

The modal fields configuration were also studied carefully and the results demonstrated compatibility of the modal structure of the EBG guide with the conventional microstrip line modes. As shown in Figure 11, the electric field is along x -axis and the magnetic field is along y -axis which proves that the fundamental mode of the EBG waveguide is a quasi-TEM mode and the EBG walls of the guiding channel can be treated as perfect magnetic conductors. Having PEC's at the top and bottom and nearly PMC's as the side walls gives rise to necessary condition for supporting quasi-TEM field as observed in Figure 11. The resemblance of the fundamental mode of the EBG guide to the guiding mode of microstripline ensures straightforward transition techniques from conventional microwave guiding structures to the EBG guide.

The group velocity, $\nu_g = d\omega/d\beta$, of the fundamental guided mode can be calculated from the linear part of its dispersion curve shown in Figure 8 [18], and is equal to 8.53×10^7 m/s. The total length of the designed structure is known, $L_t = 5.942$ cm, so the group delay time, $t_g = L_t/\nu_g$, is equal to 0.697 ns. There is a good agreement between the calculated value of the group delay time and the one calculated using CST simulation of the structure shown in Figure 10 with a value

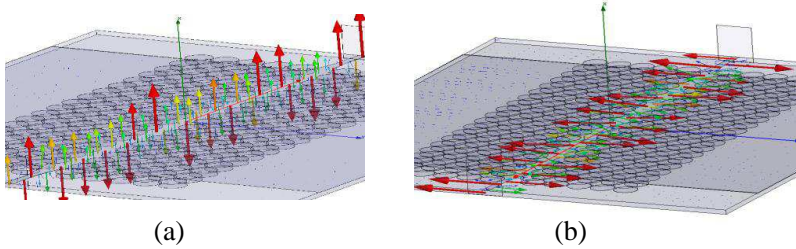


Figure 11. Fields of the EBG waveguide plotted using HFSS, (a) E -field and (b) H -field.

of 0.7113 ns. Low dispersion of the EBG guide makes a viable option for communication applications for which low frequency dispersion and modal purity is essential.

Because the fundamental guided mode within the EBG waveguide has a quasi-TEM mode nature, a square lattice of holes can be replaced by perfect magnetic conductor (PMC) sidewalls to simulate the designed structure. A spatial-domain approach [19] was used to calculate the dispersion diagram of the guided mode of the EBG waveguide as well as the corresponding dispersion diagram of a dielectric waveguide, with the same width of the middle defect region (2 mm) and using a substrate which has the same dielectric constant ($\epsilon_r = 10.2$), bounded by PMC sidewalls instead of the EBG material. Figure 12 shows the similarity between the guided modes of the dielectric waveguide and the EBG waveguide over its bandwidth, which can be used to simplify the simulation process.

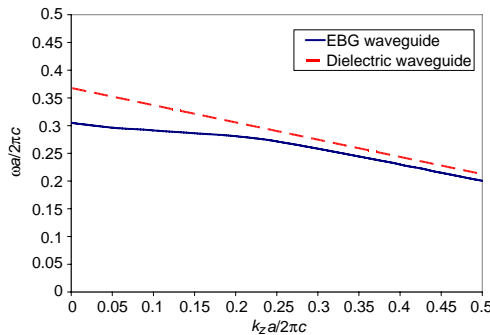


Figure 12. Calculated dispersion diagram of the EBG waveguide compared to a dielectric waveguide with the same width bounded by PMC walls.

To quantify the effect of the K-connectors on insertion loss, EBG waveguide is simulated after adding K-connectors as shown in Figure 13. K-connectors are simulated by solely considering the transition block; the connectors are not part of this simulation [20]. The discontinuity at the transition from a coax to a microstrip line is of interest in here. The two coaxial connectors are well matched and the input power is transferred to the microstrip line with insertion loss of less than 1 dB due to the K-connectors.

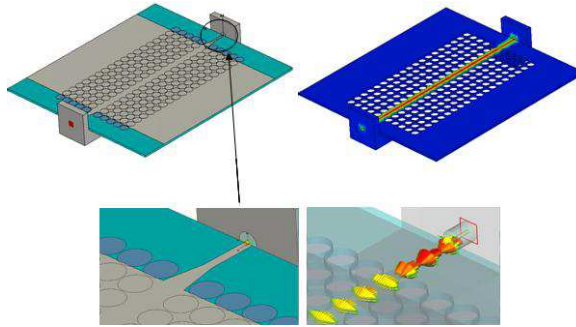


Figure 13. A simulation of EBG waveguide after adding connectors.

The designed EBG waveguide was fabricated using Rogers 6010LM dielectric material as shown in Figure 14. A microstrip line operating at 30 GHz of the same length as the EBG waveguide was fabricated using a substrate with the same dielectric constant material and was used as a benchmark to evaluate the performance of the designed EBG waveguide.

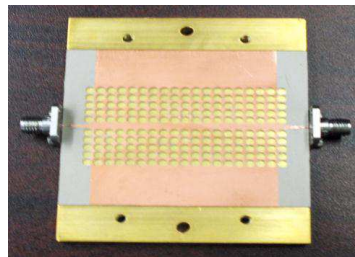


Figure 14. The fabricated EBG waveguide (top plate is not shown).

Figure 15 shows the measured data using an Anritsu 37377C vector network analyzer, along with the simulation results. It can be observed that the simulated and measured insertion loss of the microstrip line has values at the same level or less than the designed

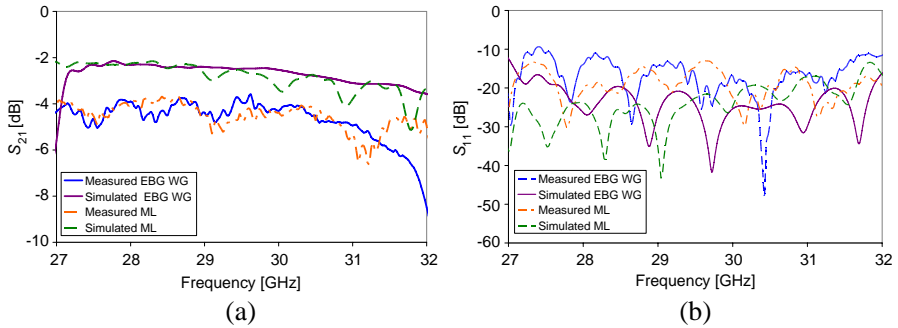


Figure 15. EBG waveguide S -parameters, (a) insertion loss and (b) return loss.

EBG waveguide. Moreover, the simulated and measured return losses of the two structures are comparable across the operating bandwidth of the EBG waveguide. The measured insertion loss of both fabricated structures, the EBG waveguide and the microstrip line, are approximately 2.0 dB below the simulated data. The 2 dB loss is deemed to be due to different factors such as conductor misalignment between K-connectors and microstrip lines, and the variations between the data sheet values and the actual values of the dielectric constant and the loss tangent. The dielectric constant of the substrate has been tabulated for 10.0 GHz in the manufacturer datasheets [21] which might be different from its value at 30 GHz as has already been noted for some other material from the same manufacturer [22]. There is a drop-off in transmission at 32 GHz due to the mini-stop band which is around 33.5 GHz as illustrated in Figure 9.

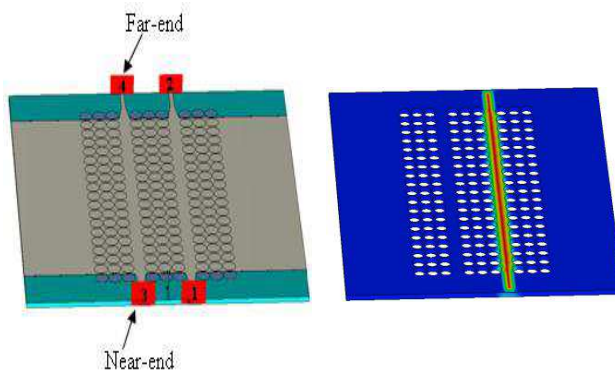


Figure 16. Two adjacent EBG waveguides.

Two adjacent EBG waveguides which have the same length as the fabricated structure (49.1 mm), separated by 3 unit cells (7.75 mm), were used as shown in Figure 16 to study the cross-talk between the EBG waveguides. Port 3 and port 4 are the near-end and far-end, respectively, as illustrated in Figure 16. To compare the performance of the EBG waveguide, a structure of two microstrip lines, which have the same length as the EBG waveguide, separated by the same distance, 7.75 mm, was simulated as well. As shown in Figures 17(b) and (c), S_{41} and S_{21} of the microstrip line seem to be constant because it has been designed using a substrate which has a high dielectric constant and a small thickness, which makes the guided wave along the microstrip line well bounded to the conductor strip especially at these operating high frequencies. The crosstalk at the near-end of the EBG waveguide is less than -25 dB from 27.5 GHz to 30 GHz which is higher than the corresponding value of the microstrip line as shown in Figure 17(a). However the microstrip line structure has better isolation because the EBG waveguide structure has a surface wave that is excited on the interface holes due to the termination of the square lattice of holes at

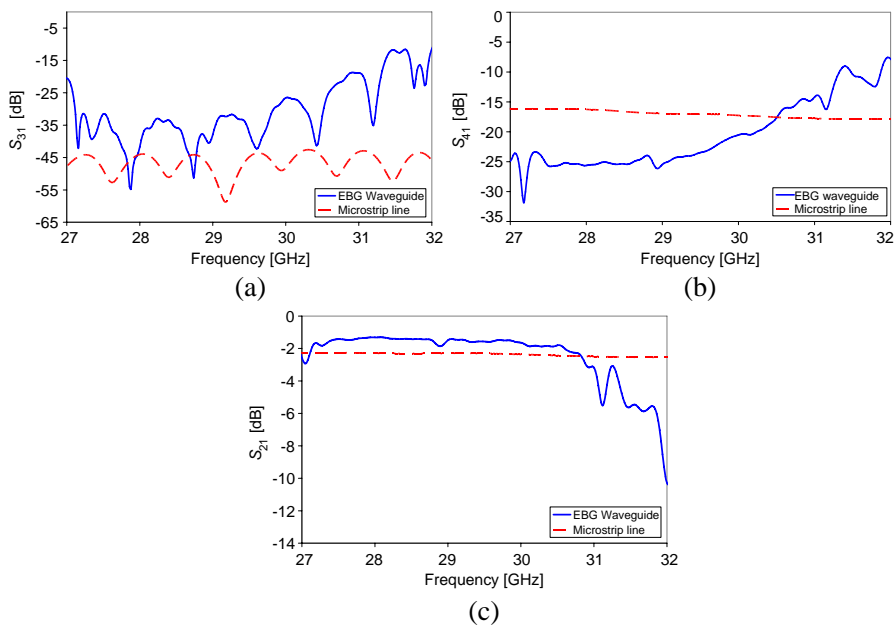


Figure 17. The simulated crosstalk and insertion loss between two adjacent waveguides compared with that of two microstrip lines, (a) near-end, (b) far-end, and (c) insertion loss.

the near end. The crosstalk at the far-end, which represents forward coupling, is less than -20 dB through the same bandwidth which is less than the corresponding coupling in the case of microstrip line structure as shown in Figure 17(b). The insertion loss of the EBG waveguide and microstrip line is also simulated and shown in Figure 17(c). As shown in this figure the insertion loss of EBG waveguide is better than microstrip line and this could be due to lower far-end cross coupling between the EBG waveguides. The advantage of the EBG for this particular coupling term is the result of the absence of surface wave contribution. The high isolation of the EBG waveguide is due to the surrounded walls which minimize the possibility of generating surface waves in contrast to its microstrip counterpart. Therefore, two adjacent EBG waveguides can be used on the same substrate with minimal crosstalk problems.

4. CONCLUSION

An EBG waveguide was thoroughly studied for application in the millimetre wave band through design and implementation of prototypes. The EBG structure was designed to achieve a stop band around 30 GHz. The band gap of this structure was calculated. This was also done to ensure that this EBG structure has a band gap at all directions of the irreducible Brillouin zone. The EBG waveguide was fabricated using the designed EBG structure and optimized to increase its bandwidth and to enhance its transmission characteristics. There is a good agreement between the obtained band structure and the stop-band calculated from the S -parameters of the designed structure before and after optimization. The insertion loss of the designed EBG waveguide is better than 2.5 dB from 27 GHz to 31.5 GHz and its return loss better than -10 dB over the same bandwidth. The simulation of the EBG waveguide using a time domain solver has demonstrated its low dispersion and nearly linear characteristics across its operating band. Also it is shown that the guided mode within the EBG waveguide is a quasi-TEM mode and its dispersion curve is linear through its bandwidth. A full wave simulation was also done to confirm the quasi-TEM nature of the guided mode. It has also been shown that PMC walls can be used to simulate the EBG material. The simulated S -parameters of two adjacent EBG waveguides show that there is good isolation, less than -20 dB from 27 GHz to 30 GHz which suggest that this EBG waveguide may have an advantage if it is used in designing millimetre wave components. At a more global level, the objective of this paper has been to contribute to the understanding of EBG structures. Such an understanding will be indispensable in

the assessment of the performance of such structures as compared to conventional structures and exploitation of their full potential in the millimetre wave band.

ACKNOWLEDGMENT

The authors would like to thank Mr. David Lee and the CRC model shop for their help in fabricating and measuring the designed structures.

REFERENCES

1. Joannopoulos, J. D., R. D. Meade, and J. N. Winn, *Photonic Crystals: Molding the Flow of Light*, Princeton Univ. Press, Princeton, NJ, 1995.
2. Zhu, S. and R. Langley, "Dual-band wearable antennas over EBG substrate," *Electronic Letters*, Vol. 43, No. 3, 141–142, Feb. 2007.
3. Radisic, V., Y. Qian, and T. Itoh, "Broadband power amplifier using dielectric photonic bandgap structure," *IEEE Microwave Guided Wave Lett.*, Vol. 8, 13–14, Jan. 1998.
4. Sharkawy, A., S. Shi, and D. W. Prather, "Electro-optical switching using coupled photonic crystal waveguides," *Optics Express*, Vol. 10, No. 20, 1048–1059, 2002.
5. Thorhauge, M., L. H. Frandsen, and P. I. Borel, "Efficient photonic crystal directional couplers," *Optics Letters*, Vol. 28, No. 17, 1525–1527, 2003.
6. Niemi, T., L. H. Frandsen, K. K. Hede, A. Harpøth, P. I. Borel, and M. Kristensen, "Wavelength-division demultiplexing using photonic crystal waveguides," *IEEE Photonics Tech. Letters*, Vol. 18, No. 1, 226–228, 2006.
7. Chien, F. S. S., Y. J. Hsu, W. F. Hsieh, and S. C. Cheng, "Dual wavelength demultiplexing by coupling and decoupling of photonic crystal waveguides," *Optics Express*, Vol. 12, No. 6, 1119–1125, 2004.
8. Frandsen, L. H., et al., "Ultralow-loss 3-dB photonic crystal waveguide splitter," *Optics Letters*, Vol. 29, No. 14, 1623–1625, 2004.
9. Johnson, S. G., P. R. Villeneuve, S. Fan, and J. D. Joannopoulos, "Linear waveguides in photonic-crystal slabs," *Physical Review B*, Vol. 62, 8212–8222, 2000..
10. Suntives, A. and R. Abhari, "Characterization of interconnects

- formed in electromagnetic bandgap substrates,” *9th IEEE Workshop on Signal Propagation on Interconnects*, 75–78, 2005.
11. Abdo, Y. S. E., M. R. Chaharmir, J. Shaker, and Y. M. M. Antar, “Efficient excitation of an EBG guide exploiting the partial bandgap of a triangular lattice of holes,” *IEEE Antennas and Wireless Propagation Letters*, Vol. 9, 167–170, 2010.
 12. Falcone, F., T. Lopetegi, M. A. G. Laso, and M. Sorolla, “Novel photonic crystal waveguide in microwave printed circuit technology,” *Microwave and Optical Technology Letters*, Vol. 34, No. 6, 462–466, Sep. 20, 2002.
 13. Gonzalo, R., I. Ederra, B. Martinez, and P. de Maagt, “Electromagnetic crystal technology for waveguides and bends at microwave frequencies,” *Electronic Letters*, Vol. 41, No. 7, 421–422, Mar. 2005.
 14. CST StudioTM Suite 2008, 2008.
 15. Adibi, A., Y. Xu, R. K. Lee, and A. Yariv, “Properties of the slab modes in photonic crystal optical waveguides,” *Journal of Lightwave Technology*, Vol. 18, No. 11, 1554–1564, Nov. 2000.
 16. Olivier, S., M. Rattier, H. Benisty, C. Weisbuch, C. J. M. Smith, R. M. De La Rue, T. F. Krauss, U. Oesterle, and R. Houdré, “Mini stopbands of a one dimensional system: The channel waveguide in a two-dimensional photonic crystal,” *Physical Review B*, Vol. 63, 113311, 2001.
 17. Deslandes, D. and K. Wu, “Integrated microstrip and rectangular waveguide in planar form,” *IEEE Microwave Wireless Compon. Lett.*, Vol. 11, No. 2, 68–70, Feb. 2001.
 18. Pozar, D. M., *Microwave Engineering*, Addison-Wesley Publishing Company, 1990.
 19. Gagnon, N., A. Ittipiboon, and A. Petosa, “Operation of a periodic structure for a microstrip line over a large frequency band,” *ANTEM/URSI*, 389–392, Jul. 2004.
 20. Anritsu, K., “V connector tips,” Anritsu Company, 2003.
 21. Rogers, RT/duroid® 6006/6010LM High Frequency Laminates Data Sheet.
 22. Birbir, F., J. Shaker, and Y. M. M. Antar, “Chebishev bandpass spatial filter composed of strip gratings,” *IEEE Transactions on Antennas and Propagation*, Vol. 56, No. 12, 3707–3713, 2008.